Life Sciences 118 (2014) 306–312

Contents lists available at ScienceDirect

Life Sciences

journal homepage: www.elsevier.com/locate/lifescie

Adipose-derived regenerative cell therapy inhibits the progression of monocrotaline-induced pulmonary hypertension in rats

Masamichi Eguchi, Satoshi Ikeda, Saburo Kusumoto, Daisuke Sato, Yuji Koide, Hiroaki Kawano, Koji Maemura *

Department of Cardiovascular Medicine, Nagasaki University Graduate School of Biomedical Sciences, Nagasaki, Japan

ARTICLE INFO

Article history:
Received 1 November 2013
Accepted 6 May 2014
Available online 20 May 2014

Keywords:
Endothelin-1
Transforming growth factor beta
Pulmonary hypertension
Adipose derived regenerative cell (ADRC)

ABSTRACT

Aims: Functional and structural changes in pulmonary vasculature characterize pulmonary arterial hypertension (PAH) and the prognosis of advanced PAH remains poor despite progress in pharmacotherapy. Adipose-derived regenerative cells (ADRCs) promote cell regeneration at pathological sites and comprise a novel therapy for ailments of various organs. We investigated the effects of ADRC therapy in rat models of monocrotaline (MCT)-induced pulmonary hypertension (PH) and the underlying mechanisms.

Main methods: Rats were assigned to Control and MCT groups without and with (M/A) intravenous transfusion of seven million ADRCs on day 7. We echocardiographically evaluated pulmonary hypertension as pulmonary artery flow acceleration time (PAAT) and deceleration (PADc). Right ventricular (RV) systolic pressure was measured by catheterization on day 28 and then pathological changes in pulmonary vessels were assessed. We analyzed PAH-associated gene expression on day 14 using real-time RT-PCR.

Key findings: Echocardiography and RV catheterization showed that ADRC therapy inhibited PH development (assessed as PAAT, PADc, and RV systolic pressure) at day 28 (MCT vs. M/A, $P < 0.05$). Pulmonary vascular remodeling was also inhibited (vessel wall thickness: MCT vs. M/A, $P < 0.01$). Messenger RNA levels of endothelin (ET) A and B receptors, ET-1 and transforming growth factor (TGF)-β increased in the lungs by MCT were suppressed by ADRCs (MCT vs. M/A, $P < 0.05$).

Significance: The development of PH was inhibited by ADRCs through suppressing changes in the expression of genes associated with ET and TGF-β systems. We believe that ADRC therapy could serve as a novel strategy for treating PH.

Introduction

Pulmonary arterial hypertension (PAH) is a debilitating chronic disorder of the lungs that is characterized by perpetually elevated blood pressure in the pulmonary vasculature (Galie et al., 2009). The cause of PAH is often idiopathic, but it can also arise secondarily due to medical conditions such as collagen disease, heart malformations or viral infections. Genetic and epigenetic risk factors have also been linked to PAH pathogenesis (Loscalzo, 2001), but, all known causes of PAH are associated with endothelial dysfunction, vasoconstriction and pulmonary vessel remodeling.

Endothelial dysfunction is an early component of the pulmonary hypertensive process, during which an imbalance is created between vasodilators such as nitric oxide (NO) and prostacyclin, and vasoconstrictors such as endothelin, thromboxane A2 and serotonin (Morrell et al., 2009). This imbalance leads to a cascade of events that results in the hyper-proliferation of pulmonary smooth muscle cells, the activation of lung fibroblasts, the induction of thrombotic mediators and inflammatory cytokine release, all of which increase vascular resistance and pressure. One factor that is associated with endothelial dysfunction and vascular impairment is the endothelin system. Endothelin-1 (ET-1), a peptide produced mainly by endothelial cells, was discovered in 1988 and it is a potent vasoconstrictor and smooth muscle cell mitogen (Yanagisawa et al., 1988). The ET-1 system is activated in both the plasma and lung tissues of patients with PAH and in animal models of pulmonary hypertension (PH).

Pulmonary arterial hypertension is refractory to most conventional pharmacological therapies. Stem cell therapy might constitute a novel treatment modality for patients with PH. Mesenchymal stem cells (MSC) are unique in that they are pluripotent and can secrete paracrine factors that improve damaged tissue (Passier and Mummery, 2003). One such novel potential therapy for PH lies within the regenerative properties of easily accessible and abundant adipose tissue-derived stem and regenerative cells (ADRCs) that can be used in real-time, autologous applications. Here, we investigated the effects of ADRC therapy on PH and explored the underlying mechanisms in a rat model of monocrotaline (MCT)-induced PH.

* Corresponding author at: Department of Cardiovascular Medicine, Nagasaki University Graduate School of Biomedical Sciences, 1-7-1 Sakamoto, Nagasaki 852-8501, Japan. Tel.: +81 95 819 7286; fax: +81 95 819 7280.
E-mail address: maemura@nagasaki-u.ac.jp (K. Maemura).

http://dx.doi.org/10.1016/j.lfs.2014.05.008

Materials and methods

Isolation of ADRCs

We isolated ADRCs from 13- to 14-week-old male Wistar rats (200–250 g) as described with minor modifications (Angelini et al., 2011; Feng et al., 2010). Briefly, inguinal subcutaneous adipose tissue was removed, minced and digested with 0.1% collagenase (Sigma-Aldrich, St. Louis, MO, USA) for 40 ± 5 min at 37 °C. The ADRC fraction was separated by centrifugation at 600 ×g for 5 min and sequentially passed through 100- and 40-μm Falcon™ cell strainers (BD Biosciences, San Jose, CA, USA). The ADRCs were washed in phosphate-buffered saline (PBS) and resuspended (7.0×10^6/mL) in PBS. Some ADRCs were labeled with the cross-linkable membrane dye CM-DiI (Invitrogen™, Carlsbad, CA, USA) as described in the manufacturer's protocol.

Flow cytometric analysis of ADRC

Adipose-derived regenerative cells resuspended in staining buffer were incubated for 10 min at 4 °C with antibodies to block non-specific binding and then for 30 min at 4 °C with CD45FITC (554878), CD31PE (555027) and CD90PE (551401) (all from BD Pharmingen, San Diego CA, USA) for flow cytometry. The cells were washed twice with cold Dulbecco's PBS, fixed using FACS Lysing Solution (BD Biosciences) and then analyzed on a FACSAria using FACSDiva software (BD Biosciences).

Colony forming unit-fibroblast (CFU-F) assay

CFU-F assay was performed as described by Hayashi et al. (2008). Briefly, ADRCs were seeded at a density of 1×10^3 nucleated cells/cm^2 in 6-well plates and incubated in Dulbecco's Modified Eagle Medium (DMEM) (Sigma-Aldrich) with 10% fetal bovine serum (FBS) (Sigma-Aldrich). Medium was changed every 3–4 days. Six days after plating, colonies were stained with Crystal Violet (Wako, Osaka, Japan) and counted. Only cell aggregates containing more than 50 cells were scored as a colony. The CFU is defined as colony number per 100 nucleated cells seeded.

Animal models

Monocrotaline (Sigma-Aldrich) was dissolved in 1 N HCl. The pH was neutralized with 1 N NaOH, and the volume was adjusted with PBS to achieve a concentration of 15 mg/mL. Eight week-old Wistar rats weighing 225–250 g (Japan SLC Inc., Shizuoka, Japan) were subcutaneously injected with a bolus of MCT (50 mg/kg) or an equal volume of PBS (Control group). All rats were weighed twice weekly during the study and analyses proceeded until 28 days after MCT or sham injection. The Experimental Animal Committee at the Biomedical Research Center Division of Comparative Medicine Center for Frontier Life Sciences at Nagasaki University approved the experimental protocols and animal care methods applied in the study.

Experimental groups

All experiments proceeded in a blinded manner to evaluate the effects of ADRC therapy. One week after MCT injection, the rats were randomly assigned to one group that received 1 mL of PBS (MCT group) or 7.0×10^6 ADRC (M/A group) via the caudal vein. Control rats received neither MCT nor ADRC (Control). Various types of cells in the range of 4.0×10^6 to 2.0×10^7 have been injected into the caudal vein as stem cell therapy for PH in previous studies (Angelini et al., 2011; Kim et al., 2012). Therefore, the amount of ADRCs injected herein was within this range.

Echocardiography

The rats were examined by transthoracic echocardiography using a ProSound Alpha 7 ultrasound device (Hitachi-ALOKA Medical, Tokyo, Japan) with a 13.0 MHz linear transducer. Pulmonary artery flow was measured using pulsed wave Doppler sonography with a sample gate of 1.0 mm at the level of the pulmonary valve but signals for pulmonary artery flow acceleration time (PAAT) and deceleration (PADc) were determined at the right ventricular outflow tract and opening and closing clicks of the pulmonary valve were avoided. We defined PAAT as the interval from onset to the maximal velocity of forward pulmonary artery flow and PADc as the first linear deceleration period after maximal velocity (Koskenvuo et al., 2010).

Measurement of right ventricular systolic pressure and hypertrophy

Twenty-eight days after MCT injection, the rats were anesthetized with isoflurane and a 3-Fr tube was inserted via the right jugular vein into the right ventricle (RV) to measure RV pressure using a PowerLab 2/26 with BP Amp (ADInstruments, Colorado Springs, CO, USA) under a closed chest. The position of the catheter in RV was confirmed by the waveform. Data were analyzed using the Chart program supplied with the Power Lab system. Right ventricular hypertrophy was assessed by weighing the RV separately from the left ventricle (LV) with the septal wall (S).

Histological studies

After measuring the RV systolic pressure, the rats were sacrificed with an overdose of pentobarbital sodium and several tissues including the lungs, heart and liver were fixed with 4% paraformaldehyde for morphological analysis. Paraffin-embedded sections were processed for hematoxylin–eosin (HE) and Elastica van Gieson stain (EVG) for optical microscopic studies. The remodeling of pulmonary arterioles was analyzed using the Sahara method (Sahara et al., 2007) in which the external diameter and medial wall thickness were measured in 30 muscular arterioles (<100 μm external diameter) per lung section using a computer-based image analysis system comprising a BZ-9000 fluorescence and optical microscope (KEYENCE, Tokyo, Japan). The ratio of medial thickness was calculated as: medial wall thickness × 2 / external diameter.

Terminal deoxynucleotidyl transferase dUTP nick end labeling (TUNEL) assays proceeded using MK500 in-situ apoptosis detection kits (Takara Bio Inc., Otsu, Shiga, Japan) according to the manufacturer's protocol. The number of TUNEL-positive cells was counted and averaged in 10 fields under a light microscope at ×200 magnification, and representative fields were photographed.

Some of the tissues were fixed with 4% formaldehyde that was increased to 30% over 4 days and then immersed in OCT compound (Sigma-Aldrich). The tissues were frozen in liquid nitrogen and stored at −80 °C. Each section was cut into 7- to 10-μm slices. The survival of ADRCs in the lung tissue was confirmed by the presence of DiI-labeled cells. Immunofluorescence staining proceeded using a 1:200 dilution of FITC-conjugated mouse monoclonal anti-rat alpha smooth muscle actin (SMA) antibody (Sigma-Aldrich) or a 1:50 dilution of mouse monoclonal anti-rat PECAM-1 (CD31) antibody (Millipore, Darmstadt, Germany) with a 1:1000 dilution of FITC-conjugated goat anti-mouse IgG antibody (Millipore). Nuclei were stained with DAPI (Vector Laboratories Inc., Burlingame, CA, USA).

Real-time reverse transcribed-polymerase chain reaction (RT-PCR)

The rats were sacrificed with an overdose of pentobarbital and the upper lung lobe was removed and immersed in RNA later for 24 h and frozen at −80 °C for PCR. The lung tissue was used for RT-PCR to analyze gene expressions.

Total RNA was isolated using RNeasy Micro kits (QIAGEN, Hilden, Germany) and cDNA was reverse transcribed using PrimeScript™ RT reagent kits (Takara Bio Inc.) as described (Vernal et al., 2008). The mRNA levels of ET-1, endothelin A (ETA) receptor, endothelin B (ETB) receptor, interleukin (IL)-6, IL-10, vascular endothelial growth factor (VEGF), hepatocyte growth factor (HGF), connective tissue growth factor (CTGF), transforming growth factor beta (TGF-β) and glyceraldehyde-3-phosphate dehydrogenase (GAPDH) were determined using real-time quantitative PCR. Forward and reverse primers were designed (Supplemental Table 1) using Primer3 (http://bioinfo.ut.ee/primer3-0.4.0/primer3). Reference gene candidates were amplified by real-time quantitative PCR using 10 μL of SYBR Premix Ex Taq (Takara Bio Inc.), 2 μL of diluted reverse transcription product, 0.4 μL of forward and reverse primer and 7.2 μL of DNase/RNase-free water in a total volume of 20 μL. Amplification proceeded in a LightCycler 480 (Roche Applied Science, Basel, Switzerland) with initial polymerase activation at 95 °C for 10 min, followed by 40 cycles of 95 °C for 15 s and 60 °C for 60 s. Thereafter, the specificity of amplicons was verified by melting curve analysis (60 °C to 95 °C). Fluorescent signals were normalized to an internal reference and the threshold cycle (Ct) was set within the PCR exponential phase. Relative gene expression levels were calculated by comparing cycle times for each target PCR. The Ct values of target mRNA were normalized by subtracting that of GAPDH to give the ΔCt value. Relative expression levels were calculated using the equation:

$$\text{relative gene expression} = 2^{-(\Delta Ctsample\ -\ \Delta Ctcontrol)}.$$

Statistical analysis

Results are expressed as means ± standard deviation. Intergroup comparisons were analyzed using one-way analysis of variance followed by Tukey's test. A P value of <0.05 was considered statistically significant. All data were statistically analyzed using Stat Flex ver. 6.0 software (Artech Ltd., Osaka, Japan).

Results

Characterization of ADRCs

The yield of fresh ADRCs isolated from pooled rat adipose tissues ($n = 8$) was $1.15 \pm 0.34 \times 10^6$/g. Flow cytometry ($N = 3$) showed that ADRCs comprised an average of 9.4% $CD45^+$ cells (blood and tissue-derived leucocytes), 1.7% cells expressed endothelial cell markers ($CD45^-/CD31^+$) (Supplemental Fig. 1B) and 18.5% expressed $CD90^+/CD45^-$ (Supplemental Fig. 1C) that are surface markers of stromal cells. We further examined the colony-forming capability of ADRCs by CFU-F assay (Supplemental Fig. 1D). The CFU-F for ADRCs was 5.7 ± 2.3/100 nucleated cells.

Gains in body weight and mortality

Gains in body weight significantly decreased in the MCT and M/A groups compared with the Control group during the study period. More weight tended to be gained by the M/A, than the MCT group (Control vs. MCT and M/A: 61.9 ± 6.0 vs. 16.8 ± 27.3 and 37.6 ± 10.9 g, $P < 0.01$ for both; MCT vs. M/A, 16.8 ± 27.3 vs. 37.6 ± 10.9 g, $P = 0.06$) (Supplemental Table 2). Three of 13 rats died in the MCT group, whereas all rats remained alive in the Control and M/A groups during the study period. However, Kaplan–Meier analysis showed no statistically significant difference in mortality rates among the three groups (data not shown).

ADRCs suppress PH induced by MCT

The rats with PH were assessed by echocardiography at baseline, and at 21 and 28 days after MCT injection. The blood flow of pulmonary arteries in the MCT group resulted in more triangular, dagger-shaped Doppler signals. The blood flow of pulmonary arteries in the M/A group was almost normal, suggesting that the high resistance in the pulmonary artery had become attenuated after cell transplantation (Fig. 1A). The PAAT was significantly shorter in the MCT, than in the Control group on days 21 and 28 (day 28: 20.5 ± 3.2 vs. 30.0 ± 4.3 ms, $P < 0.01$). Treatment with ADRCs significantly lengthened the PAAT on day 28 (MCT vs. M/A, 20.5 ± 3.2 vs. 23.7 ± 3.6 ms, $P < 0.05$). The PADc was significantly increased in the MCT, compared with the Control group on days 21 and 28 (day 28: 1434 ± 412 vs. 717 ± 193 cm/s^2; $P < 0.01$). Treatment with ADRCs significantly shortened the PADc on day 28 (MCT vs. M/A, 1434 ± 412 vs. 904 ± 229 cm/s^2, $P < 0.01$; Fig. 1B).

Right ventricular pressure was measured by catheterization in all groups on day 28 after MCT injection. Right ventricular systolic pressure was significantly elevated in the MCT, compared with the Control group (37.2 ± 5.1 vs. 20.8 ± 3.4 mm Hg, $P < 0.01$). Treatment with ADRCs inhibited this increase in RV systolic pressure (MCT vs. M/A, 37.2 ± 5.1 vs. 29.9 ± 6.6 mm Hg, $P < 0.05$; Fig. 1C). The ratio of RV/LV plus S, an index of RV hypertrophy, was elevated in the MCT, compared with the Control group (0.37 ± 0.15 vs. 0.22 ± 0.04, $P < 0.05$). However, the RV/LV plus S did not significantly differ between the MCT and M/A groups (Fig. 1D).

ADRCs improved pulmonary artery remodeling induced by MCT

In line with the hemodynamic data, HE and EVG staining confirmed that ADRC transplantation attenuated the obliterative remodeling of the small arteries that started in the lungs after MCT injection. The small arteries in the MCT group featured medial hypertrophy and a hyperplastic response in the pulmonary arterioles (Fig. 2A). The ratio of medial wall thickness to the external diameter of the pulmonary artery was significantly increased in the MCT, compared with the Control group on day 28 (0.44 ± 0.04 vs. 0.17 ± 0.04, $P < 0.01$). The ratio of medial wall thickening of the pulmonary artery was significantly decreased in the M/A group compared with the MCT group on day 28 (0.31 ± 0.05 vs. 0.44 ± 0.04, $P < 0.01$; Fig. 2B).

We counted the apoptotic cells in lung tissues (Supplemental Fig. 2A) and found significantly more apoptotic cells in the MCT, than in the Control group (2.3 ± 1.2 vs. 0.4 ± 0.2, $P < 0.05$). However, the number of apoptotic cells did not significantly differ between the MCT and M/A groups (Supplemental Fig. 2B).

Identification of transplanted ADRC

DiI-positive cells in the lungs that emitting red fluorescence at seven days after ADRC transplantation (Fig. 2C and F) were often located near αSMA- (Fig. 2D) and CD31- (Fig. 2G) positive cells that emitted green fluorescence. We counted 4.52 ± 2.56 ADRCs in one ×200 power magnification field. However, the cells emitting red and green fluorescence were not colocalized (Fig. 2E and H), suggesting that most intravenously implanted ADRCs did not differentiate into vascular endothelial or smooth muscle cells in vivo. Red fluorescence was also emitted by the liver but not the heart of ADRC treated rats.

Gene expression analysis in the lung

On day 14 after MCT injection, mRNA levels of ET system components (ET-1, ETA receptor and ETB receptor) and TGF-β in the lungs were significantly higher in the MCT, than the Control group ($P < 0.05$; Fig. 3A–D). These increases were inhibited by ADRCs (MCT vs. M/A, $P < 0.05$; Fig. 3A–D). Levels of IL-6 mRNA were increased in the MCT, compared with the Control group, but they were not inhibited by ADRCs (Fig. 3E). On the other hand, MCT did not significantly change mRNA levels of IL-10, CTGF, HGF and VEGF, whereas the level of IL-10 mRNA was increased in the M/A, compared with the Control group (Fig. 3F–I).

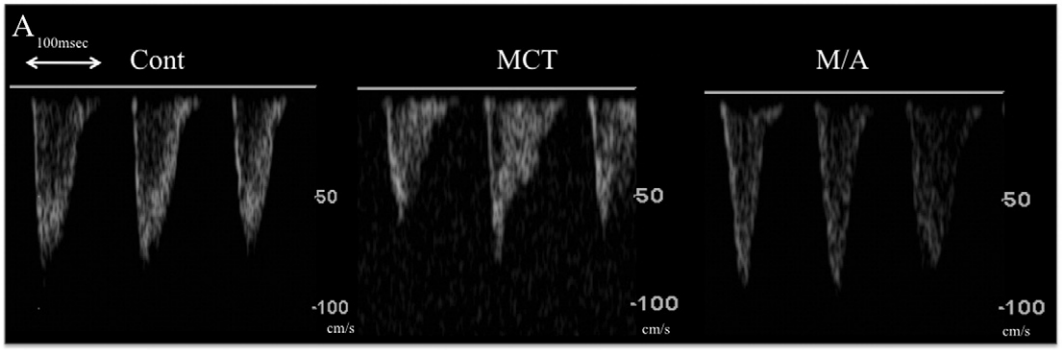

B

		day0	day21	day28
PAAT	Cont	31.0±3.3	29.5±3.3	30.0±4.3 †
(msec)	MCT	31.6±3.7	23.7±4.2	20.5±3.2 ‡
	M/A	31.2±3.3	26.8±3.1	23.7±3.6
PADc	Cont	741±53	658±117 †	717±193 †
(cm/s^2)	MCT	648±116	1088±460 ‡	1434±412 §
	M/A	765±106	728±147	904±229

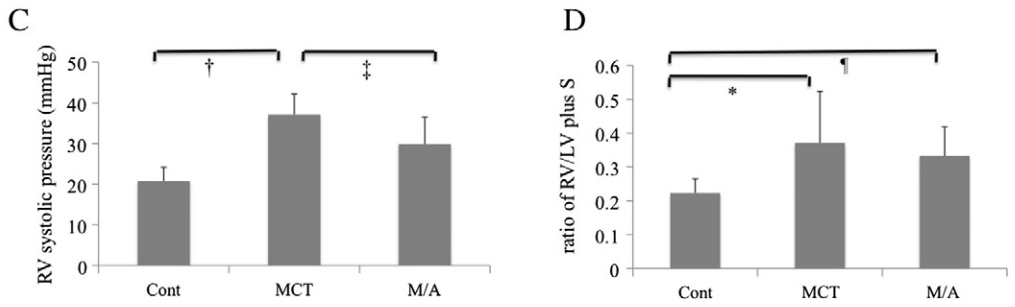

Fig. 1. Therapy with ADRCs attenuated pulmonary hypertension in MCT-induced lung injury. (A) PAAT and PADc as surrogates for mean pulmonary artery pressure measured by Pulsed Wave-Doppler echocardiography. Representative flow pattern of pulmonary artery. (B) PAAT and PADc after MCT injection in Control (n = 10), MCT (n = 12) and M/A (n = 13) groups. (C) RV systolic pressure at 28 days after MCT injection (n = 10). (D) Ratio of RV weight/left ventricular plus septal weight (n = 10). Data are shown as means ± SEM. *P < 0.05, †P < 0.01 MCT vs. Cont; ‡P < 0.05, §P < 0.01 MCT vs. M/A; ¶P < 0.01 M/A vs. Cont.

Discussion

We investigated the effects of ADRC therapy in a rat model of PH induced by MCT. We found that ADRC therapy significantly inhibited the progression of hemodynamic parameters assessed by right heart catheterization and echocardiography, vascular remodeling and the gene expression of ET-1, ETA receptor, ETB receptor and TGF-β in the lungs.

Regenerative and gene therapy has recently become a global research focus, but stem cell research remains in its infancy, and treatment for PH has not yet been standardized. Therefore, further experimental investigations into a safe and practical strategy for treating PH are urgently required. Several studies have assessed the ability of stem cell therapy using MSC and endothelial progenitor cells to protect against PH. For example, Zhao et al. (2005) found that rat endothelial progenitor cells exerted a protective effect in a rat model of PH induced by MCT and that this effect was enhanced when the cells were transfected with the eNOS gene. Luan et al. (2012) also found a protective effect of MSC though a paracrine mechanism in a PH model induced by high flow. We also found that ADRC therapy protects against PH, but we did not directly compare ADRC therapy with other types of stem cell therapy such as endothelial progenitor cells or MSC, and thus whether or not ADRC therapy is more effective than these therapies remains a topic for future study. However, large quantities of ADRC, that do not require expansion ex vivo, can be isolated by minimally invasive liposuction thus rendering them an appealing and practical source for immediate cell-based therapies (Fraser et al., 2004; Strem and Hedrick, 2005). The development of PH was inhibited by ADRCs at least in part, through inhibiting the expression of genes associated with the ET system. Plasma levels of ET-1 are elevated in patients with PH (Stewart et al., 1991), and ET-1 levels correlate with pulmonary arterial pressure, pulmonary artery oxygen saturation and pulmonary vascular resistance (Cacoub et al., 1997; Giaid et al., 1993). Levels of ET-1 are also increased in the lungs of animal models of PH (Kim et al., 2012). Levels of ET-1 can be modulated by TGF-β in human pulmonary microvascular endothelial cells in vitro and the enhanced stimulatory effects of TGF-β might lead to the vascular abnormalities associated with PH (Newman et al., 2008). Lambers et al. (2013) reported that ET-1 also activates pulmonary artery smooth muscle cells, and that the synergistic effects of ET-1 and TGF-β mediate vascular remodeling though ERK1/2 MAPK kinesis. Since we detected ADRCs in the lung at day 14 and hemodynamic differences between days 14 and 21, we considered that ADRCs exerted therapeutic effects during the early phase of MCT-induced PH. Therefore, we assessed mRNA concentrations of the cytokines and growth factors that are involved in the process of PH development on day 14 using the RT-PCR. We then examined histology of the lung and heart tissues at day 28. The present study found that ADRC therapy might attenuate vascular remodeling by reducing the expression of genes associated with both the TGF-β and ET systems.

The ADRC population comprised various types of cells. About 41.6% and 3.4% of fresh ADRCs express mesenchymal and endothelial cell markers, respectively (Feng et al., 2010) and 18.5% and 1.7% of our ADRC population expressed surface markers of stromal cells and

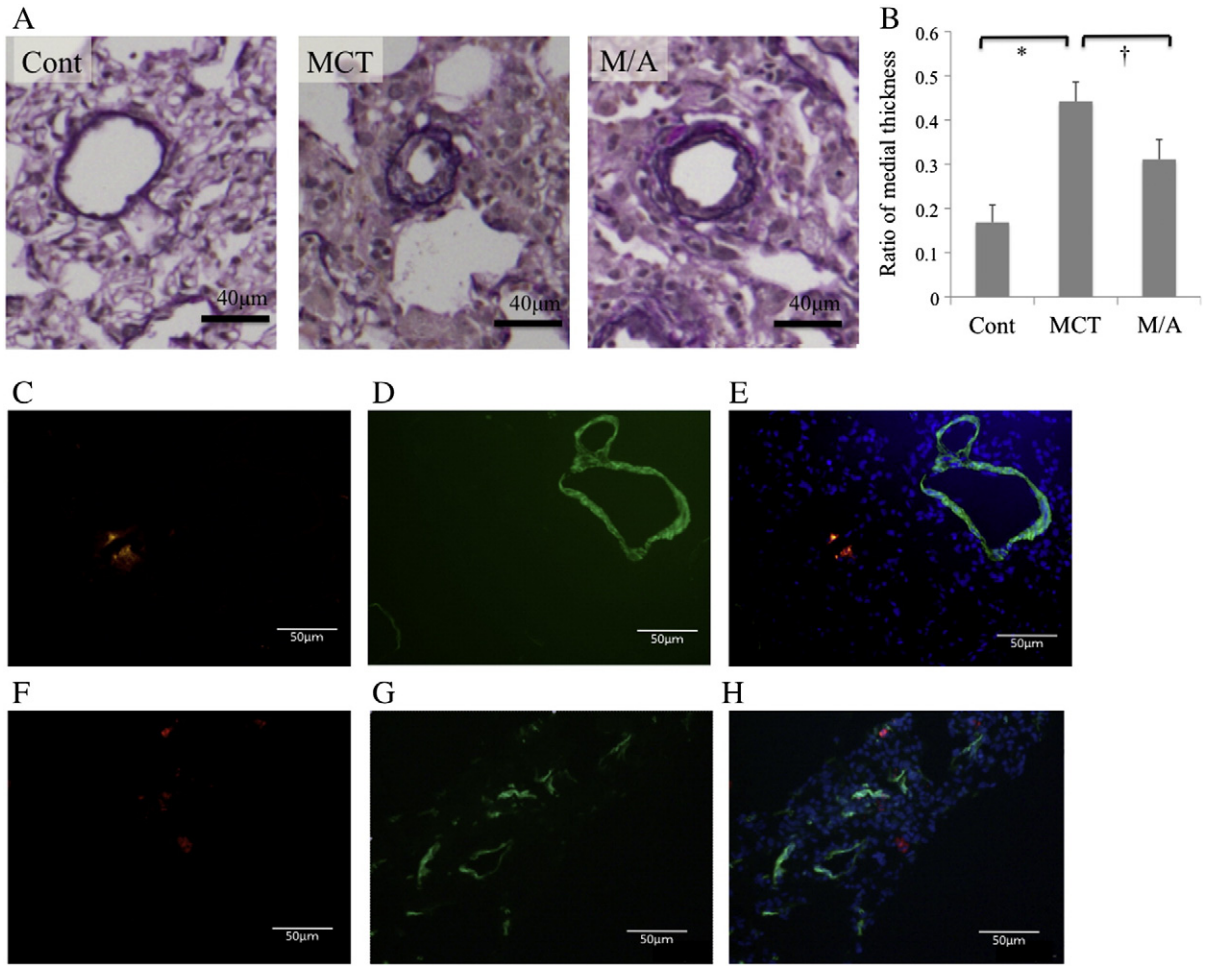

Fig. 2. Effect of ADRCs on MCT-induced vessel wall thickness and identification of transplanted ADRCs. (A) Representative microphotographs of pulmonary vessels from Control, MCT and M/A groups (n = 5–6 per group; scale bar, 40 μm). (B) Analysis and quantitation of vessel wall thickness. Data are shown as means ± SEM. *P < 0.01 MCT vs. Cont; †P < 0.01 MCT vs. M/A. (C) and (F) Labeled ADRCs around lung vessels at seven days after transplantation. (N = 4; scale bar, 50 μm). (D) Green αSMA staining indicates smooth muscle cells; (G) CD31 (green) staining indicates endothelial cells; (E) and (H) merged images of DAPI staining (blue) indicate nuclei.

endothelial cell markers, respectively. Moreover 7% of ADRCs were reported to be stem cells (Hayashi et al., 2008) and 5% of our ADRCs were considered as stem cells from CFU-F assay. Thus, we consider that our population of ADRCs was similar to previous reports.

Several investigators have described a paracrine mechanism of ADRC therapy in various experimental models (Harada et al., 2013; Suganuma et al., 2013). The expression of several growth factors such as VEGF, HGF and insulin-like growth factor (IGF)-1 by ADRCs after acute myocardial infarction in rats indicated that these cells promote angiogenesis and exert anti-apoptotic/necrotic effects via a paracrine mechanism (Schenke-Layland et al., 2009). Furthermore, ADRCs downregulate the expression of inflammation-related genes such as IL-6 and chemokine (C-X-C motif) ligand 2 (CXCL2), and significantly reduce inflammation after acute kidney injury in rats (Feng et al., 2010).

Angelini et al. (2011) reported that stem cell therapy using adipose tissue stromal vascular fraction (SVF) induced positive pulmonary vascular remodeling, and improved neurohormonal profiles as well as hemodynamic effects in rat models of PH. That study also found that treatment with SVF prevents increases in levels of inflammatory serum cytokines. These results agree with our study. In addition, we also examined the gene expressions associated with TGF-β and ET systems in the lung tissue. Then we found that ADRC therapy attenuated vascular remodeling though reducing the expression of genes associated with the TGF-β and ET systems without changing angiogenesis. The levels of IL-6 were significantly increased in the MCT group and those of IL-10 were increased in the M/A group compared with the Control group, suggesting the anti-inflammatory effect of ADRCs. However, precisely how ADRC suppresses the expression of genes associated with the TGF-β and ET systems remains unknown.

The significance of apoptosis in the pathogenesis or treatment of PH is controversial. Li et al. (2014) reported that apoptosis of endothelial cells in the lung tissue increased in MCT-induced PH, which triggered smooth muscle cell growth, suggesting that apoptosis of endothelial cells plays a role in the development of PH. Akagi et al. (2013) reported that high-dose prostaglandin (PG) I2 induces apoptosis in pulmonary artery smooth muscle cells from the patients with IPAH in association with beneficial effects of PGI2. Although apoptotic cells were increased in the MCT group, we could not detect the anti-apoptotic effect of ADRCs in this study. Thus, the anti-PH effect of ARDCs may not be mediated through the anti-apoptotic effect.

This study has several limitations. The dose of injected MCT (50 mg/kg) was relatively low to minimize animal mortality. Several studies that have used 60 mg/kg of MCT induced a higher RV pressure and a higher RV/LV + S ratio than we did (Baber et al., 2007; Frasch et al., 1999; Lee et al., 2013). Thus, the amount of pressure overload in our model might not be sufficient to cause RV remodeling. Therefore, the increase in the RV/LV + S ratio in the MCT group was small and we could not show the effects of ADRCs on RV remodeling.

We delivered ADRCs relatively soon after injecting MCT to show that ADRC therapy could inhibit the progression of PH. Considering the

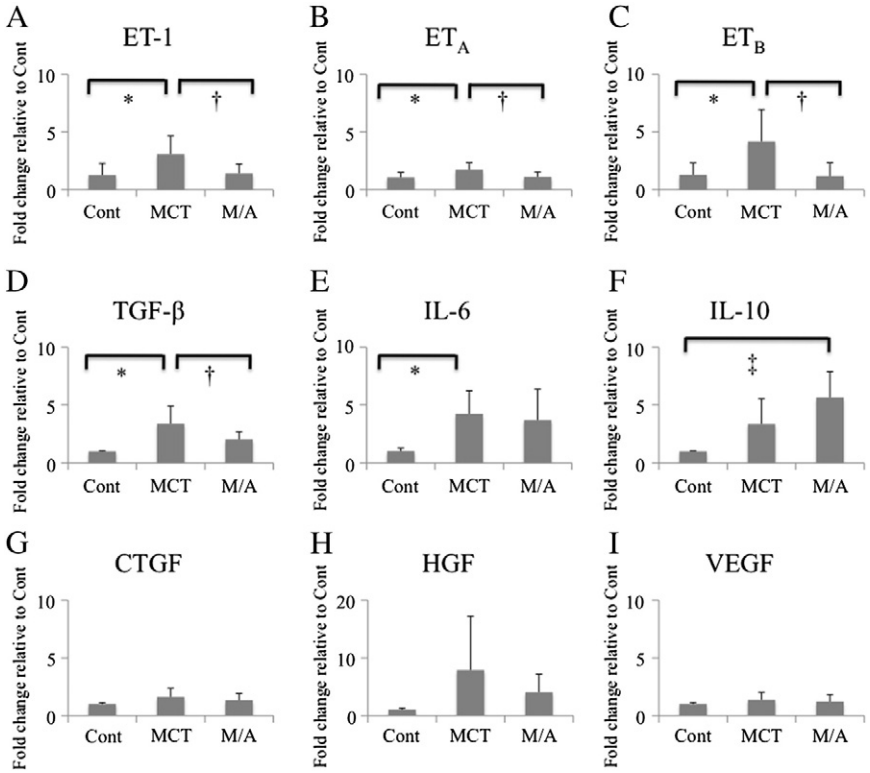

Fig. 3. Messenger RNA levels in the lung. Messenger RNA levels were normalized to GAPDH and are shown as ratios to those in Control lungs (n = 6). Values are shown as means ± SEM. *P < 0.05 MCT vs. Cont; †P < 0.05 M/A vs. MCT; ‡P < 0.05 M/A vs. Control.

clinical situation, however, the therapeutic effects of ADRCs delivered at various times after PH established should also be confirmed.

The major limitation of this study is that the rat model of MCT-induced PH partly differs from human PAH. Other rodent models of PAH (Abe et al., 2010) and larger animals should be tested to open a translational investigation of ADRC therapy on human pulmonary arterial hypertension.

Lastly, we showed that transplanted ADRCs persisted in the lungs for at least up to seven days after transplantation. Most of them were located in the stroma and a few were incorporated into the pulmonary vessels. How long the transplanted ADRCs can survive in the lung and maintain a paracrine effect remains unknown. We believe that transfusion with ADRCs derived from GFP-positive rats instead of DiI staining will help to address this issue in a future study.

Conclusion

The intravenous administration of ADRCs into rats with MCT-induced PH inhibited PH development by suppressing changes in the expression of genes associated with the TGF-β and ET systems. These results indicate that uncultured autologous ADRCs could serve as a novel strategy for treating PH.

Conflict of interest statement

None declared.

Acknowledgments

We are grateful to Dr. I. Shimokawa (Department of Investigative Pathology, Unit of Basic Medical Sciences, Nagasaki University Graduate School of Biomedical Sciences) for providing assistance with the histological analysis. We also thank Ms. S. Usui and Ms S. Toda for excellent technical assistance.

This study was supported by a grant for medical research from the Alumni Association of Nagasaki University School of Medicine.

Appendix A. Supplementary data

Supplementary data to this article can be found online at http://dx.doi.org/10.1016/j.lfs.2014.05.008.

References

Abe K, Toba M, Alzoubi A, et al. Formation of plexiform lesions in experimental severe pulmonary arterial hypertension. Circulation 2010;121(25):2747–54.
Akagi S, Nakamura K, Matsubara H, et al. Prostaglandin I2 induces apoptosis via upregulation of Fas ligand in pulmonary artery smooth muscle cells from patients with idiopathic pulmonary arterial hypertension. Int J Cardiol 2013;165(3):499–505.
Angelini A, Castellani C, Ravara B, et al. Stem-cell therapy in an experimental model of pulmonary hypertension and right heart failure: role of paracrine and neurohormonal milieu in the remodeling process. J Heart Lung Transplant 2011;30(11):1281–93.
Baber SR, Deng W, Master RG, et al. Intratracheal mesenchymal stem cell administration attenuates monocrotaline-induced pulmonary hypertension and endothelial dysfunction. Am J Physiol Heart Circ Physiol 2007;292(2):H1120–8.
Cacoub P, Dorent R, Nataf P, et al. Endothelin-1 in the lungs of patients with pulmonary hypertension. Cardiovasc Res 1997;33(1):196–200.
Feng Z, Ting J, Alfonso Z, et al. Fresh and cryopreserved, uncultured adipose tissue-derived stem and regenerative cells ameliorate ischemia–reperfusion-induced acute kidney injury. Nephrol Dial Transplant 2010;25(12):3874–84.
Frasch HF, Marshall C, Marshall BE. Endothelin-1 is elevated in monocrotaline pulmonary hypertension. Am J Physiol 1999;276(2 Pt 1):L304–10.
Fraser JK, Schreiber RE, Zuk PA, et al. Adult stem cell therapy for the heart. Int J Biochem Cell Biol 2004;36(4):658–66.
Galie N, Hoeper MM, Humbert M, et al. Guidelines for the diagnosis and treatment of pulmonary hypertension: the Task Force for the Diagnosis and Treatment of Pulmonary Hypertension of the European Society of Cardiology (ESC) and the European Respiratory Society (ERS), endorsed by the International Society of Heart and Lung Transplantation (ISHLT). Eur Heart J 2009;30(20):2493–537.
Giaid A, Yanagisawa M, Langleben D, et al. Expression of endothelin-1 in the lungs of patients with pulmonary hypertension. N Engl J Med 1993;328(24):1732–9.
Harada Y, Yamamoto Y, Tsujimoto S, et al. Transplantation of freshly isolated adipose tissue-derived regenerative cells enhances angiogenesis in a murine model of hind limb ischemia. Biomed Res 2013;34(1):23–9.
Hayashi O, Katsube Y, Hirose M, et al. Comparison of osteogenic ability of rat mesenchymal stem cells from bone marrow, periosteum, and adipose tissue. Calcif Tissue Int 2008;82(3):238–47.

Kim KC, Lee HR, Kim SJ, et al. Changes of gene expression after bone marrow cell transfusion in rats with monocrotaline-induced pulmonary hypertension. J Korean Med Sci 2012;27(6):605–13.
Koskenvuo JW, Mirsky R, Zhang Y, et al. A comparison of echocardiography to invasive measurement in the evaluation of pulmonary arterial hypertension in a rat model. Int J Cardiovasc Imaging 2010;26(5):509–18.
Lambers C, Roth M, Zhong J, et al. The interaction of endothelin-1 and TGF-beta1 mediates vascular cell remodeling. PLoS ONE 2013;8(8):e73399.
Lee FY, Lu HI, Zhen YY, et al. Benefit of combined therapy with nicorandil and colchicine in preventing monocrotaline-induced rat pulmonary arterial hypertension. Eur J Pharm Sci 2013;50(3–4):372–84.
Li L, Wei C, Kim IK, et al. Inhibition of nuclear factor-kappaB in the lungs prevents monocrotaline-induced pulmonary hypertension in mice. Hypertension 2014; 63(6):1260–9.
Loscalzo J. Genetic clues to the cause of primary pulmonary hypertension. N Engl J Med 2001;345(5):367–71.
Luan Y, Zhang X, Kong F, et al. Mesenchymal stem cell prevention of vascular remodeling in high flow-induced pulmonary hypertension through a paracrine mechanism. Int Immunopharmacol 2012;14(4):432–7.
Morrell NW, Adnot S, Archer SL, et al. Cellular and molecular basis of pulmonary arterial hypertension. J Am Coll Cardiol 2009;54(1 Suppl):S20–31.
Newman JH, Phillips III JA, Loyd JE. Narrative review: the enigma of pulmonary arterial hypertension: new insights from genetic studies. Ann Intern Med 2008;148(4): 278–83.
Passier R, Mummery C. Origin and use of embryonic and adult stem cells in differentiation and tissue repair. Cardiovasc Res 2003;58(2):324–35.
Sahara M, Sata M, Morita T, et al. Diverse contribution of bone marrow-derived cells to vascular remodeling associated with pulmonary arterial hypertension and arterial neointimal formation. Circulation 2007;115(4):509–17.
Schenke-Layland K, Strem BM, Jordan MC, et al. Adipose tissue-derived cells improve cardiac function following myocardial infarction. J Surg Res 2009;153(2):217–23.
Stewart DJ, Levy RD, Cernacek P, et al. Increased plasma endothelin-1 in pulmonary hypertension: marker or mediator of disease? Ann Intern Med 1991;114(6):464–9.
Strem BM, Hedrick MH. The growing importance of fat in regenerative medicine. Trends Biotechnol 2005;23(2):64–6.
Suganuma S, Tada K, Hayashi K, et al. Uncultured adipose-derived regenerative cells promote peripheral nerve regeneration. J Orthop Sci 2013;18(1):145–51.
Vernal R, Velasquez E, Gamonal J, et al. Expression of proinflammatory cytokines in osteoarthritis of the temporomandibular joint. Arch Oral Biol 2008;53(10):910–5.
Yanagisawa M, Kurihara H, Kimura S, et al. A novel potent vasoconstrictor peptide produced by vascular endothelial cells. Nature 1988;332(6163):411–5.
Zhao YD, Courtman DW, Deng Y, et al. Rescue of monocrotaline-induced pulmonary arterial hypertension using bone marrow-derived endothelial-like progenitor cells: efficacy of combined cell and eNOS gene therapy in established disease. Circ Res 2005; 96(4):442–50.